

Optically Induced Mask-Controlled Time-Variable Periodic Microwave Structures

Walter Platte, Stefan Ruppik, and Manfred Guetschow

Abstract—Based on the distributed Bragg reflection performance of stationary light-induced periodic microwave structures, this paper presents different kinds of modified arrangements for the generation of time-variable plasma gratings. Initial experimental investigations concentrate on the alteration of the grating period as a function of time. It is realized by a photographic film slot-array mask of linearly graded slot width transversely moved across an light-emitting-diode-excited photosensitive coplanar waveguide. The characterization of such a mask-tuned filter configuration requires special measuring procedures, which are illustrated and discussed in detail. The principle of operation demonstrated at X -band frequencies offers the potential of being extended to the submillimeter-wave and low-terahertz ranges.

Index Terms—Optical-microwave interactions, optically induced microwave filters, time-variable periodic microwave structures, tunable plasma gratings.

I. INTRODUCTION

OPTICAL-MICROWAVE interaction has become a topic of growing interest during the last 20 years. Among various kinds of optoelectronic microwave control, only the frequency-selective method of employing a finite periodically photoexcited section (PPS) within a semiconductor-based waveguide offers the advantage of very low excitation levels needed. The PPS acts as a plasma-induced grating exhibiting the well-known leaky-wave and stopband phenomena [1]–[5]. Since the local period can be changed by altering the illumination pattern, a PPS can be developed for optically controlled millimeter-wave beam-steering antennas [6] and distributed Bragg reflection (DBR) microwave filters of stepwise variable center frequency [7], or can be used for microwave measurements of an effective dielectric constant of semiconductor waveguides [8].

Usually, a PPS is generated by continuous-wave (CW) illumination, e.g., through a slot-array overlay mask [3], [9], or by means of a pattern-controlled fiber bundle array [7]. Moreover, the spatial distribution of the light-induced carrier density (or photoconductivity) within the semiconductor material is independent of time. Thus, the plasma grating is operated under steady-state conditions. The resulting microwave performance of such a stationary PPS has been analyzed and optimized in detail with special regard to the frequency-dependent reflection and transmission characteristics [1]–[5], [10]–[13].

Manuscript received April 22, 1999. This work was supported by the Gesellschaft der Freunde und Förderer der Universität der Bundeswehr Hamburg e. V.

The authors are with the University of the Federal Armed Forces Hamburg, Hamburg D-22043, Germany (e-mail: HFTTechnik@unibw-hamburg.de).

Publisher Item Identifier S 0018-9480(00)03752-2.

As an interesting extension of this static PPS technique, this paper presents the basic principles of creating a time-variable plasma grating and outlines the actual application potential. Furthermore, first experimental investigations on an optically induced mask-tuned DBR microwave filter are reported, in which the PPS was generated by CW LED excitation of a ceramic-based CdS–CdSe coplanar waveguide (CPW) through a photographic film slot-array mask of graded slot width, transversely moved across the CPW surface. The very promising results should serve as a stimulus for further research on the field of time-variable plasma gratings, possibly taking aim at tunable-filter applications for the submillimeter-wave or even quasi-optical regions.

II. BASIC PRINCIPLES OF TIME-VARIABLE PPS GENERATION

Referring to the foundations for PPS generation [1]–[5], the microwave performance of the plasma grating can be determined from the one-dimensional distribution of excess carrier density across the longitudinal waveguide axis z , i.e., the direction of wave propagation. When supposing, for simplicity, a symmetric photoexcitation where the length l_1 of the excited sections is equal to the length l_2 of the dark sections and, moreover, l_1 is assumed to be much greater than the ambipolar diffusion length L_a of the light-induced carriers, the static PPS is characterized by the abrupt-profile distribution of photoconductivity $\Delta\sigma(z)$, shown in Fig. 1 as a dashed line.

The most familiar way for creating a time-dependent grating is to apply pulsed or modulated light sources. In this case, the photoconductivity profile and its change in magnitude may be imagined as an array of equidistant plasma teeth moving up and down as a function of time [see Fig. 1(a)]. The local position of the grating structure within the waveguide slab as well as the width of all teeth and their distance to each other remain constant in time. The corresponding experimental arrangement is shown in Fig. 2(a) where pulsed illumination through a locally fixed slot-array mask of uniform slot width generates the time-variant PPS. Of course, this method is trivial and does not need further discussion. Nevertheless, such a very special arrangement can be successfully used for some kinds of pulse-induced waveform generation by employing suitable pulse-modulated lasers.

The second kind of time-variable PPS is characterized by a CW-induced grating exhibiting plasma sections of constant photoconductivity and time-invariant local period Λ (with $\Lambda = l_1 + l_2$), as shown in Fig. 1(b). The complete PPS now travels within the waveguide either into or against the direction of wave propagation, altering the position z_c of the grating

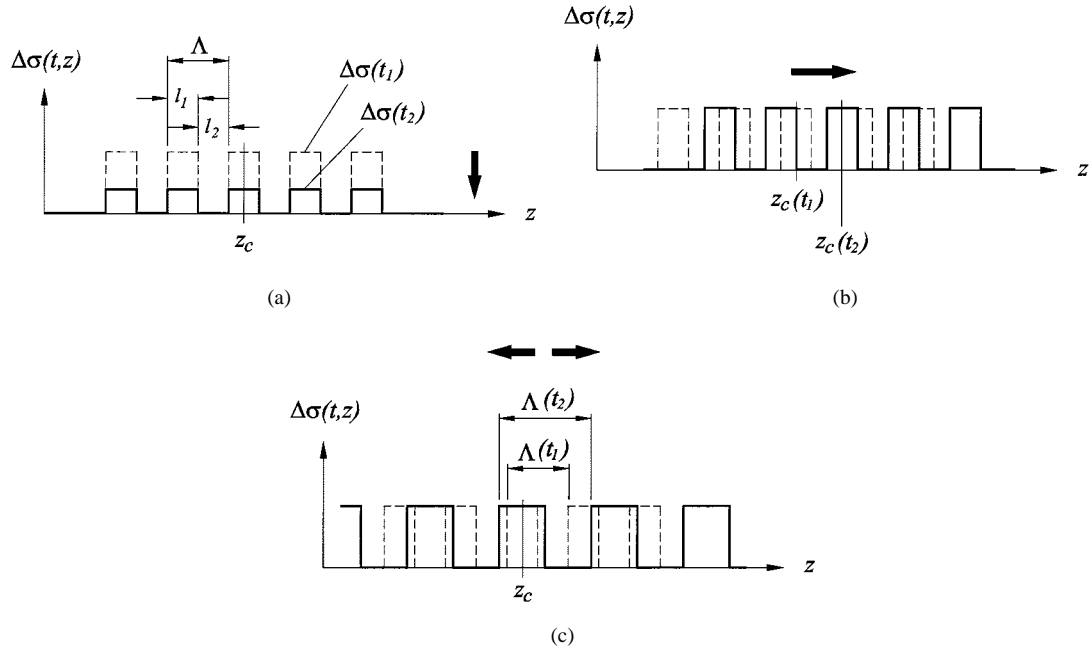


Fig. 1. Locally periodic abrupt-profile distribution of photoconductivity $\Delta\sigma(t, z)$ with time-dependent variation of: (a) photoconductivity $\Delta\sigma(t)$, (b) grating center position $z_c(t)$, and (c) local period $\Lambda(t)$.

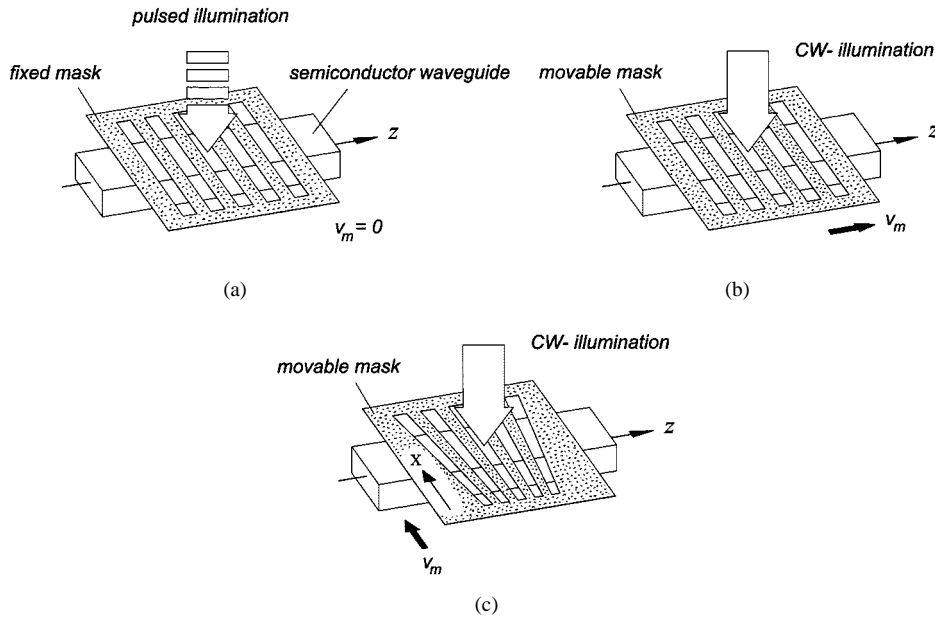


Fig. 2. Experimental arrangements for creating a time-variable plasma grating through: (a) a fixed mask under pulsed illumination, (b) a longitudinally moved mask under CW illumination, and (c) a transversely moved mask of graded slot width under CW illumination.

center, e.g., from $z_c(t_1)$ to $z_c(t_2)$. One possible experimental setup is sketched in Fig. 2(b) where a CW-illuminated slot-array mask of uniform slot width is moved with constant velocity v_m parallel to the z -axis, very close to the waveguide surface. In this case, a Doppler frequency shift of the reflected microwave signal occurs, which can be utilized for optoelectronic single-sideband (SSB) generation. This technique could possibly substitute other (e.g., mechanical [14]) methods of SSB generation in the millimeter- and submillimeter-wave region. Of course, the actual propagation velocity of the plasma grating is governed by the effective carrier lifetime of semiconductor

material used. From this, true high-speed operation is expected to become reality as soon as improved conditional artificial dielectric materials [15] are available.

The third most interesting type of time-variant PPS also exhibits a CW-induced grating of constant photoconductivity in which, however, the local period Λ is a function of time. The grating structure dilates and contracts with respect to its fixed center position z_c [see Fig. 1(c)]. This method of operation can easily be realized in practice by applying a CW-illuminated slot-array mask of (e.g., linearly) graded slot width, transversely moved across the waveguide [see Fig. 2(c)], whereby a

continuous sweep of the grating center frequency f_c is achieved. Since f_c is inversely proportional to the corresponding center wavelength λ_c and to the period Λ , respectively, a linear graduation of slot width across the longitudinal axis of the mask (x -axis) results in a linear sweep of $\lambda_c(t)$, supposing constant speed of the mask. On the other hand, a linear sweep of $f_c(t)$ is usually preferred, which can be realized by a $1/x$ graduation of slot width. It is obvious from physical aspects that semiconductor waveguides of sufficiently low carrier lifetime are required for operating such a mask-tuned DBR filter at high sweep rates. At the current state of knowledge, this latter type of time-variable PPS seems to offer the most promising application potential, especially concerning future submillimeter-wave and low-terahertz technology, which may be inferred from basic experiments described in Section III.

III. MASK-TUNED PPS IN A CPW CONFIGURATION

Tunable filters are important components of electrical and optical systems, and a nearly infinite variety of special filter arrangements has been successfully applied in the field of electrical and optical engineering. In the lower range of the electromagnetic spectrum, which extends from the RF bands up to the millimeter-wave region, the tuning of filters and resonators is usually performed by means of electronic circuitry incorporating, e.g., varactors and YIG elements. In the upper region, where optical frequencies dominate, tunable filters are mostly realized on the basis of purely optical techniques, which utilize complex arrangements of lenses and gratings such like that in an optical monochromator.

Up to now, there is no practicable method for setting up a tunable filter configuration for the submillimeter-wave and quasi-optical region, although this intermediate range of electromagnetic spectrum has become a subject of growing interest in the last decade [16]. Referring to the aforementioned purely electronic and optical methods of filter tuning, it seems quite consistent to introduce an optoelectronic solution (e.g., in the form of a time-variable PPS with a movable graded-slotwidth mask) for tunable-filter applications in the 0.1–4-THz range. However, because corresponding measuring equipment is not currently available, both the principle and feasibility of mask-controlled PPS tuning are demonstrated at microwave frequencies.

The first ten-stage mask-controlled PPS structure consisted of a closed-loop photographic film tape of 490-mm total length and 120-mm width, which was transversely moved across the CPW, as shown in Fig. 3. For easier realization of swept-center-frequency measurements, the film tape exhibited up to four identical slot arrays, arranged one after another, each characterized by a linearly graded slot width l_1 (with $2.5 \text{ mm} \leq l_1 \leq 4.0 \text{ mm}$) and the strip width l_2 equal to l_1 (Fig. 4). Owing to a speed-controlled drive motor, the tape velocity v_m could be adjusted at values ranging from 5 to 110 mm/s. Thus, the corresponding sweep time T_{sw} amounted to $22 \text{ s} \geq T_{\text{sw}} \geq 1 \text{ s}$.

Uniform CW illumination was supplied from a 200-W halogen lamp generating a white-light illuminance of about 10 klx at the CPW surface. The test CPW consisted of a ceramic substrate measuring 6 in \times 4 in \times 0.025 in with a polycrystalline CdS(70%)–CdSe(30%) coating of 4- μm

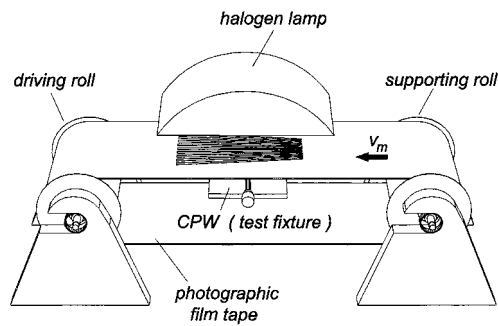


Fig. 3. Sketch of mask-tuned PPS filter arrangement based on a uniformly traveling closed-loop tape of photographic film.

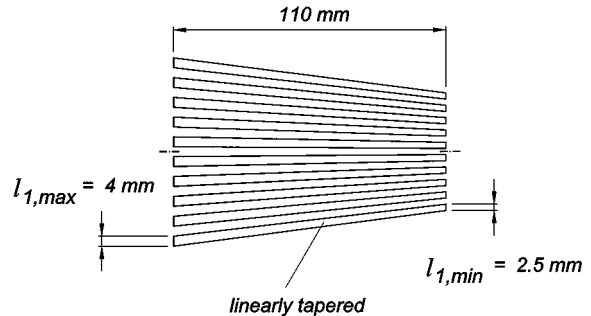


Fig. 4. Actual dimensions of the slot-array mask used for the generation of a tunable ten-stage plasma grating within a semiconductor CPW.

thickness evaporated. The effective excess carrier lifetime τ_{eff} was in the order of 10 ms at 10 klx, thus, the quasi-static condition $\tau_{\text{eff}} \ll T_{\text{sw}}$ applied. 2- μm -thick aluminum electrodes [13] formed a CPW of strip width $S = 2.20 \text{ mm}$ and slot width $W = 0.47 \text{ mm}$, resulting in a characteristic waveguide impedance of $Z_l = 49 \Omega$ and a relative effective dielectric constant of $\epsilon_{\text{re}} = 4.50$ at X-band frequencies, with the film mask overlaid. Based on a special vector subtraction procedure [3], [7], the measurements of a light-induced reflection coefficient Γ_N from an N -stage plasma grating were performed by means of a vector network analyzer (HP 8510 C) operated in the gating mode. Failing a suitable measuring technique for pick up and visual indication of the dynamic filter characteristics during a sweep of center frequency f_c , substitutionally the static ($v_m = 0$) DBR performance was acquired by a stepwise sliding of the graded-slotwidth mask, recording the swept-frequency reflection spectrum $|\Gamma_N(f)|$ for each of the 16 f_c -specific mask positions of equal (6.875 mm) spacing [17]. The results are presented in Fig. 5.

The relationship between $|\Gamma_N|$, l_1 , and f of a mask-tuned PPS arrangement can be illustrated by the tuned-filter reflection mountains $|\Gamma_N(l_1, f)|$ rising over the l_1-f plane. Supposing that the uniform motion of the mask (of linearly graded slot width) produces a time-proportional reduction of slot width l_1 from $l_{1,\text{max}}$ to $l_{1,\text{min}}$ [see Fig. 6(a)] along with a resultant nonlinear variation of f_c as a function of time and, on the other hand, the network analyzer generates a time-proportional sweep, i.e., a linear ramp, of signal frequency f from f_A to f_B [see Fig. 6(b)], the ridge of the reflection mountains (curve a) [see Fig. 6(c)] traces the nonlinear (dashed) curve b in the ground plane. In other words, curve b represents the locus

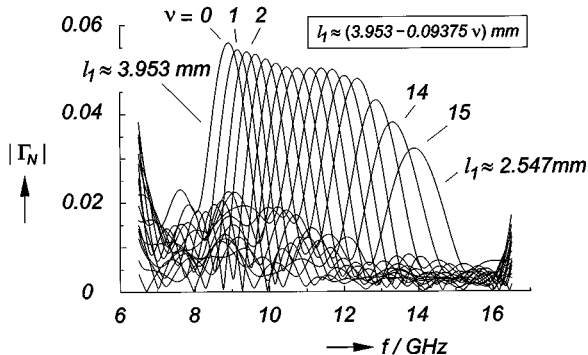


Fig. 5. All-in-one presentation of the stepwise measured (static) swept-frequency reflection spectra $|\Gamma_N(f)|$ with slot width l_1 as parameter.

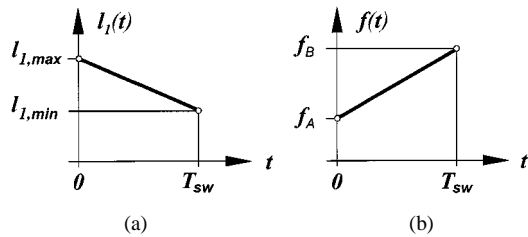
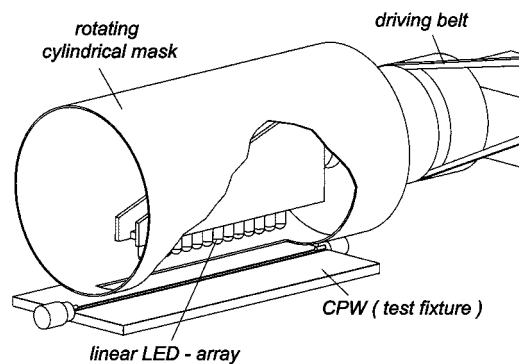
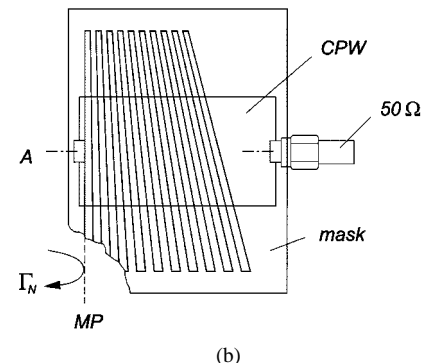


Fig. 6. Illustrative interpretation of the operating method of a mask-tuned PPS arrangement. (a) Sweep of slot width $l_1(t)$ by uniform mask motion. (b) Sweep of signal frequency $f(t)$ by network analyzer. (c) Resultant reflection mountains $|\Gamma_N(l_1, f)|$. ($f_A = f_{c,A}$ and $f_B = f_{c,B}$ for simplicity).

where the individual f_c value that follows from the actual mask position is equal to the signal frequency. For simplicity, Fig. 6(c) is based on the assumption of equal sweep intervals, i.e., $f_A = f_{c,A}$ and $f_B = f_{c,B}$, where $f_{c,A} = f_c(l_{1,\max})$ and $f_{c,B} = f_c(l_{1,\min})$. In comparison with the straight line c , which would be obtained from a time-proportional sweep of f_c , there is a difference between the corresponding f_c values, of course, which can easily be determined from a quite simple analysis. As a result, the relative maximum difference δ occurs at half the sweep time T_{sw} associated with $l_{1,\delta} = (l_{1,\min} + l_{1,\max})/2$, and amounts to $\delta = -(f_{c,A} - f_{c,B})^2/(f_{c,A} + f_{c,B})^2$ at $f_{c,\delta} = 2f_{c,A}f_{c,B}/(f_{c,A} + f_{c,B})$. Thus, the maximum-reflection performance $|\Gamma_N(f_c)|$ for a time-variable f_c cannot be measured by means of a synchronous sweep of $l_1(t)$ and $f(t)$. Instead of this, the reflection mountains can be composed by a computer-aided stacking of discrete sectional planes,



(a)



(b)

Fig. 7. (a) Improved mask-tuned PPS filter arrangement based on a rotating cylindrical film mask under white-light CW illumination from a linear 17-element LED-array. (b) Modified slot-array mask and its alignment with respect to the CPW axis (A) and the measuring plane (MP).

each generated either by swept-frequency measurements in the form of $|\Gamma_N(f)|$ at a fixed mask position (section A) or by moved-mask measurements in the form of $|\Gamma_N(l_1)|$ at a fixed signal frequency (section B). Based on this knowledge, the envelope of the swept-frequency filter curves shown in Fig. 5 can be recognized as the projection of curve a on the $|\Gamma_N| - f$ plane for $v_m = 0$. Moreover, it is well understood from physical aspects that $|\Gamma_N(l_1, f)|$ will decrease with growing v_m . This characteristic behavior, which obviously is of some importance for future tuned-PPS applications, can only be revealed by section-B measurements and subsequent evaluation of the corresponding envelope (i.e., the projection of curve a on the $|\Gamma_N| - l_1$ plane) as a function of v_m .

In a second experiment [18], an improved mask-controlled PPS arrangement [see Fig. 7(a)] with a rotating cylindrical mask of 135-mm length and 80-mm diameter was used. This photographic film drum exhibited a single slightly modified slot array [see Fig. 7(b)], thereby eliminating the undesired quasi-periodic amplitude modulation of $|\Gamma_N(f_c)|$ from the former mask (Fig. 4) caused by the l_1 -dependent (and, hence, f_c -dependent) offset length of line section between the first obliquely positioned light-induced plasma discontinuity and the measuring plane (MP). The peripheral velocity could be altered within the range $20 \text{ mm/s} \leq v_m \leq 80 \text{ mm/s}$. Uniform CW illumination was supplied from a linear 17-element LED array (Nichia NSPW-510 BS) generating a white-light illuminance of about 12 klx at the CPW surface. The optimized test CPW was specified as follows: $6 \text{ in} \times 4 \text{ in} \times 0.025 \text{ in}$

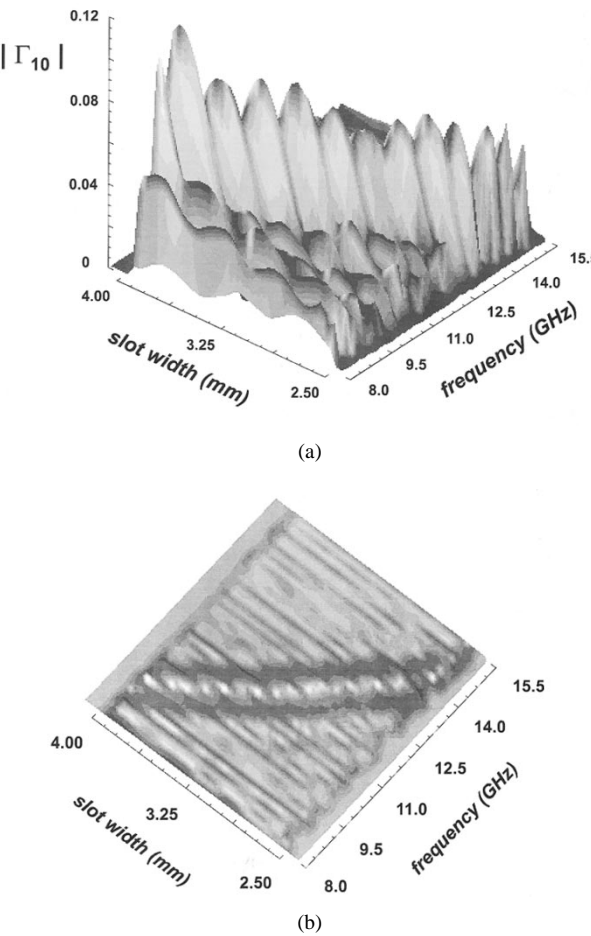


Fig. 8. Measured reflection mountains $|\Gamma_{10}(l_1, f)|$ of the LED-excited rotating-mask-controlled ten-stage PPS arrangement ($T_{sw} = 6.3$ s). (a) Three-dimensional surface plot. (b) Top view.

ceramic substrate, 4- μ m CdS(70%)-CdSe(30%) coating, 2- μ m aluminum electrodes, $S = 1.680$ mm, $W = 0.465$ mm, and $Z_l = 50 \Omega$. As a result, Fig. 8(a) shows the corresponding reflection mountains $|\Gamma_{10}(l_1, f)|$ composed by 5000 equidistant section-B measurements at $T_{sw} = 6.3$ s within the frequency range of $8.0 \text{ GHz} \leq f \leq 15.5 \text{ GHz}$. The ripple of the ridge curve is due to an imperfect matched load of the test CPW. Its periodicity of $F \approx 500 \text{ MHz}$ at 12 GHz verifies the well-known swept-frequency mismatch relation $F = c_0/2L\sqrt{\epsilon_{re}}$ with the total CPW length $L = 148$ mm, $\epsilon_{re} = 4.08$, and the velocity of light in free space c_0 . The top view [see Fig. 8(b)] clearly exhibits the nonlinear ridge trace in the l_1-f plane [see also Fig. 6(c)].

IV. CONCLUDING REMARKS

This experimental approach of mask-controlled PPS tuning has been successfully carried out under the quasi-static abrupt-profile conditions $T_{sw} \gg \tau_{eff}$ and $l_1 \gg L_a$, confirming the basic ideas up to the mark. The next step of development toward higher frequencies currently concentrates on an LED-excited cylindrical-mask CPW configuration of about five times smaller dimensions, applying gold-coated silicon substrates of about 10- μ s effective carrier lifetime [19]. From this, considerably higher sweep rates along with truly abrupt plasma discontinuities

and smaller filter bandwidths will become possible; however, associated with lower photosensitivity and reduced DBR efficiency [3], [20]. In addition, substantial improvement of the measuring procedure, especially for pick up and recording of the dynamic filter characteristics, can be achieved by a continuous $1/x$ graduation of slot width suited to produce a time-proportional sweep of center frequency synchronously to the signal frequency ramp. Moreover, it is well understood that an extension to much higher frequencies implies the use of purely dielectric waveguides which, e.g., could open an interesting potential of novel mask-tuned PPS beam-steering applications.

Intensive efforts are currently made to substitute the vector network analyzer and its frequency-discrete synthesized measuring technique by an analog method revived, in particular, with respect to future investigations of tuned-PPS arrangements for the submillimeter-wave and low-terahertz ranges. At present, the input reflection coefficient of a single test specimen under the dark-CPW condition and that under the moved-mask excited-CPW condition are measured successively (followed by the vector subtraction procedure), which is prone to experimental error [3]. Therefore, much better measuring accuracy is expected from a pair of identical CPW's on a common substrate where one of it is operated under the dark-CPW condition, while the other works as the mask-tuned PPS, both terminated in optimized nonreflecting loads. Measurements of both input reflection coefficients as well as the subtraction procedure could be performed simultaneously, e.g., by means of a suitable power divider together with a differential hybrid unit.

In conclusion, it should be noted that the tuning of PPS devices by a moved mask is only considered an incipient state of research, which obviously ensures quick and easy laboratory tests. In an advanced stage, however, the alteration of the grating period could be accomplished by a laser-fed micromodule lens-mirror system or, as a more futuristic idea, by a flat two-dimensional pattern-controlled LED array configured as an integral part of the waveguide.

REFERENCES

- [1] M. Matsumoto, M. Tsutsumi, and N. Kumagai, "Bragg reflection characteristics of millimeter waves in a periodically plasma-induced semiconductor waveguide," *IEEE Trans. Microwave Theory Tech.*, vol. MTT-34, pp. 406-411, Apr. 1986.
- [2] —, "Radiation of millimeter waves from a leaky dielectric waveguide with a light-induced grating layer," *IEEE Trans. Microwave Theory Tech.*, vol. MTT-35, pp. 1033-1042, Nov. 1987.
- [3] W. Platte, "Periodic-structure photoexcitation of a silicon coplanar waveguide for selective optoelectronic microwave control," *IEEE Trans. Microwave Theory Tech.*, vol. 38, pp. 638-646, May 1990.
- [4] V. A. Manasson, L. S. Sadovnik, A. Mousessian, and D. B. Rutledge, "Millimeter wave diffraction by a photoinduced plasma grating," *IEEE Trans. Microwave Theory Tech.*, vol. 43, pp. 2288-2290, Sept. 1995.
- [5] A. Alphones and M. Tsutsumi, "Leaky wave radiation from a periodically photoexcited semiconductor slab waveguide," *IEEE Trans. Microwave Theory Tech.*, vol. 43, pp. 2435-2441, Sept. 1995.
- [6] V. A. Manasson, L. S. Sadovnik, V. A. Yerishin, and D. Marker, "An optically controlled millimeter wave beam-steering antenna based on a novel architecture," *IEEE Trans. Microwave Theory Tech.*, vol. 45, pp. 1497-1500, Aug. 1997.
- [7] W. Platte, "LED-induced DBR microwave filter with fiber-optically controlled change of center frequency via photoconductivity gratings," *IEEE Trans. Microwave Theory Tech.*, vol. 39, pp. 359-363, Feb. 1991.
- [8] —, "Microwave measurements of effective dielectric constant of semiconductor waveguides via periodic-structure photoexcitation," *IEEE Trans. Instrum. Meas.*, vol. 46, pp. 717-721, June 1997.

- [9] W. Platte and W. Barrasch, "High-reflection 30 GHz grating structure optically induced in a CdS film coplanar waveguide on a ceramic substrate," *Electron. Lett.*, vol. 31, pp. 400–401, 1995.
- [10] W. Platte, "Spectral dependence of light-induced microwave reflection coefficient from optoelectronic waveguide gratings," *IEEE Trans. Microwave Theory Tech.*, vol. 43, pp. 106–111, Jan. 1995.
- [11] —, "Best-case reflection analysis of low-loss excited plasma gratings," *Frequenz*, vol. 50, pp. 178–180, 1996.
- [12] —, "Scattering parameter analysis of light-induced periodic microwave structures," *Frequenz*, vol. 52, pp. 187–190, 1998.
- [13] —, "CdS–CdSe–Al₂O₃-based photosensitive coplanar waveguides for optically controlled microwave and millimeter wave components" (in German), *Frequenz*, vol. 53, pp. 46–50, 1999.
- [14] N. C. Luhmann, "Instrumentation and techniques for plasma diagnostics: An overview," in *Infrared and Millimeter Waves*, K. J. Button, Ed., New York: Academic, 1979, vol. 2, Instrumentation, pp. 1–65.
- [15] H. Grebel and M. Jimenez, "Conditional artificial dielectrics: Phase and amplitude response at microwave frequencies," *Proc. Inst. Elect. Eng.*, pt. J, vol. 140, pp. 232–236, 1993.
- [16] H. H. Brand, J. Brune, A. J. Harth, R. H. Janker, M. G. Maerz, S. L. Martius, D. P. Steup, and B. G. Stoeckel, "Terahertz research at the Erlangen university laboratories for high frequency technology," in *5th Int. Space Terahertz Technol. Symp. Dig.*, Ann Arbor, MI, 1994, pp. 1–26.
- [17] M. Roepel, S. Ruppik, and W. Platte, "Geometry variable DBR filter masks," Univ. Federal Armed Forces Hamburg, Hamburg, Germany, Internal Rep. HFT-D141, 1997.
- [18] G. Kissel, S. Ruppik, and W. Platte, "Frequency tuned DBR filter," Univ. Federal Armed Forces Hamburg, Hamburg, Germany, Internal Rep. HFT-D144, 1998.
- [19] T. Fickenscher, "Optimization of optoelectronic microwave and millimeter wave DBR waveguide filters based on silicon substrates," Ph.D. dissertation (in German), Dept. Elect. Eng., Univ. Federal Armed Forces Hamburg, Hamburg, Germany, 1997.
- [20] W. Platte, "Optimum carrier lifetime of semiconductor substrate in optoelectronic microwave grating structures," *Proc. Inst. Elect. Eng.*, pt. J, vol. 142, pp. 197–201, 1995.



Walter Platte was born in Remscheid-Lennep, Germany, on January 24, 1943. He received the Dipl.-Ing. degree in electrical engineering from the Technical University of Aachen, Aachen, Germany, in 1968, and the Dr.-Ing. degree in electrical engineering and the Habilitation degree ("venia legendi") from the University of Erlangen-Nuernberg, Erlangen, Germany, in 1975 and 1986, respectively.

From 1968 to 1969, he was with AEG-Telefunken, Ulm, Germany, where he was involved with Ku-band radar instrumentation and measurement, in particular, Doppler-radar moving-target simulators. From 1969 to 1990, he was with the Department of High-Frequency Techniques, University of Erlangen-Nuernberg, as a Research Assistant, Senior Assistant, and Adjunct Staff Member (Privat-Dozent), where he was engaged in research on laser-controlled microwave integrated circuit (MIC) and millimeter-wave components, optoelectronics, and optical communications. Since October 1990, he has been a Professor of electrical engineering and Head of the Department of High-Frequency and Optoelectronic Engineering, University of the Federal Armed Forces Hamburg, Hamburg, Germany. His research interests include optical techniques for microwave and millimeter-wave applications, lightwave technology, fiber sensors, and electromagnetic compatibility.

Dr. Platte is a member of the Verband Deutscher Elektrotechniker (VDE). He was awarded the 1977 Annual Prize presented by the Nachrichtentechnische Gesellschaft (NTG) and the 1987 Finkelnburg Habilitation Prize presented by the University of Erlangen-Nuernberg.



Stefan Ruppik was born in Herne, Germany, on February 21, 1970. He received the Dipl.-Ing. degree in electrical engineering from the University of the Federal Armed Forces Hamburg, Hamburg, Germany, in 1994, and is currently working toward the Ph.D. degree at the University of the Federal Armed Forces Hamburg.

From 1994 to 1997, he was with the German Electronic Warfare Center, Trier, Germany, where he was involved in the development of new technologies of Airborne Electronic Countermeasures. Since October 1997, he has been a Research Assistant in the Department of High Frequency and Optoelectronic Engineering, University of the Federal Armed Forces Hamburg. He joined the German Air Force in June, 1989, and currently holds the rank of captain. His research interests are focused on the development of optically tuned microwave and millimeter-wave DBR CPW filters based on CdS–CdSe substrates.



Manfred Guetschow was born in Hamburg, Germany, on August 30, 1949. He received the technician degree in electrical engineering from the Berufsforschungswerk des DGB Hamburg, Hamburg, Germany, in 1974.

From 1974 to 1977, he was with Radarleit/Philips as a Specialist in sea-based target illumination radars. Since 1977, he has been a Technician Specialist in the Department of High Frequency and Optoelectronic Engineering, University of the Federal Armed Forces Hamburg, Hamburg, Germany, where he is engaged in precision mechanical and optoelectronic technology development.

in precision mechanical and optoelectronic technology development.